JGR Atmospheres

RESEARCH ARTICLE
10.1029/2018JD030045

Characteristics of Satellite Sampling Errors in Total Precipitable Water from SSMIS, HIRS, and COSMIC Observations

Yunheng Xue[1,2,3], Jun Li[2], W. Paul Menzel[2], Eva Borbas[2], Shu-Peng Ho[4], Zhenglong Li[2], and Jinlong Li[2]

[1]Institute of Atmospheric Physics, Chinese Academy of Sciences, Beijing, China, [2]Cooperative Institute for Meteorological Satellite Studies, University of Wisconsin-Madison, Madison, WI, USA, [3]University of Chinese Academy of Sciences, Beijing, China, [4]Center for Satellite Applications and Research, NOAA, College Park, MD, USA

Key Points:
- Sampling differences in COSMIC, SSMIS, and HIRS observations largely explain observed differences between associated TPW time series
- Sampling in COSMIC, SSMIS, and HIRS has different characteristics; sampling errors in HIRS are significantly correlated with TPW variability
- Sampling errors can be reduced by averaging multisensor sampling; more factors should be considered when merging real satellite data

Correspondence to:
J. Li,
jun.li@ssec.wisc.edu

Citation:
Xue, Y., Li, J., Menzel, W. P., Borbas, E., Ho, S.-P., Li, Z., & Li, J. (2019). Characteristics of satellite sampling errors in total precipitable water from SSMIS, HIRS, and COSMIC observations. *Journal of Geophysical Research: Atmospheres*, *124*, 6966–6981. https://doi.org/10.1029/2018JD030045

Received 22 NOV 2018
Accepted 9 JUN 2019
Accepted article online 20 JUN 2019
Published online 4 JUL 2019

Abstract This study quantifies the characteristics of different satellite sampling errors in the time series of total precipitable water (TPW) derived from Constellation System for Meteorology, Ionosphere, and Climate (COSMIC) radio occultation, Special Sensor Microwave Imager Sounder (SSMIS), and High-resolution Infrared Radiation Sounder (HIRS) during the overlapping time period of January 2007 to December 2013. Gap-free data from ERA5 reanalysis of the European Centre for Medium Range Weather Forecasts are used as reference values. All TPW data are first compared with microwave radiometer measurements from Atmospheric Radiation Measurement Program. In general, they are consistent, with all their regression coefficients being greater than 0.77. Discrepancies in global TPW time series can be mainly attributed to the inherent sampling errors of these three different satellite remote sensing systems. COSMIC has small sampling errors in higher latitudes. But it has scarce samples in tropical regions, which leads to a large sampling error of 3.00 mm in the estimation of global TPW. Sampling in SSMIS is more uniform with mean errors less than 0.5 mm. But the sampling is only over the ocean. Sampling errors in HIRS are larger in tropics and north subtropical areas due to clear sky biased sampling. Moreover, it is significantly correlated with the variability of TPW, whereas the sampling error in COSMIC is less influenced by TPW. Sampling errors will be reduced and more consistent global TPW time series will be derived by simply combining the multisensor samplings together.

1. Introduction

In recent decades, meteorological satellites are playing an important role in weather forecasting and climate monitoring (Kelly, 1997; Menzel et al., 1998, 2018; Purdom & Menzel, 1996). They are widely recognized as an efficient tool for monitoring and tracking water vapor changes (Ferraro et al., 2005; Ho et al., 2007; Huang et al., 2013; John & Soden, 2007; Stephens et al., 1993; Trenberth et al., 2005). The changes of global water vapor are critical for understanding the associated precipitation, cloud radiative effects, and global warming (Soden et al., 2002; Soden & Held, 2006; Wagner et al., 2006). In addition, changes in water vapor also influence the energy budget of the Earth through the large amount of latent heat (Bosilovich et al., 2011; Marks et al., 2008).

In the past years, the passive microwave instruments, for example, the Special Sensor Microwave Imager, the Special Sensor Microwave Imager Sounder (SSMIS), and the infrared satellite sensors, for example, the High-Resolution Infrared Radiation Sounder (HIRS), the Atmospheric Infrared Sounder (AIRS) are often utilized to monitor global total precipitable water vapor (TPW) changes (Chen & Liu, 2016; Iacono et al., 2003; Kawanishi et al., 2003; Mears et al., 2011; Mears, Smith, & Wentz, 2015; Mears, Wang, et al., 2015; Shi & Bates, 2011; Wentz, 1997). The TPW, also known as integrated water vapor (IWV), is a quantitative measurement of water vapor in the atmosphere. The variation of monthly mean TPW is often used for model evaluation and climate study (Ho et al., 2012; van de Berg et al., 1991). Recently, new active global positioning system radio occultation (GPS RO) measurements have emerged and are more widely used in water vapor researches (Anthes et al., 2000, 2008; Ho et al., 2007, 2010; Kursinski & Hajj, 2001). In these studies, TPW products from single remote sensing technique is usually validated against ground-based observations, atmospheric reanalysis, or another satellite data. They are then used to analyze the water vapor changes in different regions and different time periods. Since the satellite observations were well validated by other

independent data sets, the climate studies using these observations might be convincing. However, when space-time averages of TPW are calculated, satellite observations will inherently introduce an error in space and time called sampling error. Some possible reasons are temporal gaps in the observations caused by the orbit, missing samples in some specific meteorological conditions due to the limitation of sensing techniques.

Different satellite measurements have different inherent sampling patterns, and each has its own characteristics. For instance, the infrared sensors can provide high-quality profiles but are always limited to clear sky conditions (Allan et al., 2003; Erlick & Ramaswamy, 2003; Sohn et al., 2006). While microwave imagers can provide data under cloudy conditions, they can only retrieve accurate data over ocean due to the complexity of land surface emissivity. And for the GPS-RO data, although it has all weather observations both over land and ocean, its horizontal resolution is very coarse, which is about 200 km (Ho et al., 2017; Teng et al., 2013). Actually, no single sensing technique can completely provide homogeneous data products across the whole globe and under all weather conditions with high frequency and accuracy (Ho et al., 2017; Ho & Peng, 2018). Therefore, the inherent sampling error of satellite data is inevitable in global study. However, it has not yet been adequately clarified.

Previous studies have found the importance of sampling errors in satellite data. Mears et al. (2018) indicated that there are several uncertainties in satellite TPW data like systematic errors in retrieval algorithm, random errors in observations, intersatellite calibration uncertainties and spatial-temporal sampling biases, and so on. However, when constructing the long-term variation in TPW, the random errors and systematic errors do not contribute substantially and can be ignored in most cases, whereas the sampling errors and possible uncertainty in intersatellite calibration will influence the determination of long-term TPW changes. Other studies also show that sampling errors may cause the estimates of climate variables to be uncertain. For example, Ho et al. (2017) validated the accuracy of Constellation System for Meteorology, Ionosphere, and Climate (COSMIC) data with collocated microwave radiometer measurements. But finally, a much higher global TPW trend was got with this validated data set. It was higher than previous studies by about a factor of 4 to 6. When they investigated the results in more details, they found that the COSMIC data used are highly biased toward higher latitudes (40–60°N and 40–65°S). So, even though COSMIC data have global coverage, the trend derived from COSMIC is more of a trend in subtropical area where storm tracks exist rather than a global one. John et al. (2011) studied the clear-sky biases in infrared estimates of upper tropospheric humidity and found that the maximum clear-sky bias is up to −30% relative humidity over convectively active areas. So it is important to understand the advantages and limitations of each satellite data record before using them for climate studies. And it is necessary to figure out how and to what extent different sampling will influence climate studies to avoid any misinterpretation and spurious estimation. However, there are not many studies based on monthly time scales to demonstrate the sampling errors in TPW from different sensors.

Therefore, the objective of this study is to analyze and clarify the sampling errors in monthly mean TPW time series from different satellite measurements. It should be noted that the purpose of this study is not to evaluate the overall accuracy of real satellite data but to understand and characterize the sampling errors. In order to achieve this goal, a subsampling study is conducted, similar to the work described in Mears et al. (2018). In their study, the error introduced by microwave sampling was analyzed by using the actual sampling pattern for each satellite to subsample 6-hourly TPW values obtained from the National Center for Environmental Prediction Global Data Assimilation System final analysis. In this study, the ERA5 reanalysis data with high spatial and temporal resolutions are used as the reference data set to analyze the characteristics of sampling errors from three different satellite measurements in the same time period.

This article is organized as follows: section 2 describes the data sets and methods used in this study, section 3 gives the analysis and result of sampling errors in each satellite measurements, section 4 provides the discussion about the potential improvement caused by using multiple samplings, and conclusions are summarized in section 5.

2. Methodologies and Data

2.1. Methodologies

In this study, sampling errors in microwave imagers from the SSMIS, infrared data from HIRS, and GPS RO data from COSMIC are investigated simultaneously in the overlapping time period from the year of 2007 to

2013. As we mentioned above, there are a variety of differences in different remote sensing systems, so it is difficult to directly compare their sampling. Another data set should be used as a reference which needs to be relatively accurate with high spatial and temporal resolutions for describing TPW changes. In particular, it should provide uniform (gap-free) data coverage. Atmospheric reanalysis data can provide global coverage and homogeneous long-term TPW record. Additionally, all major atmospheric reanalysis data sets have assimilated a variety of observations, such as that from radiosondes, ground-based GPS, diverse satellites, buoys, and so on. Nevertheless, reanalysis data are not perfect. There are still some issues like incorrect physical processing in the numerical weather prediction model, uncertainty in radiative transfer operator in cloudy skies for assimilation (e.g., Li et al., 2016), misrepresentation of diurnal cycle of variables like clouds over some regions, and so on. A higher-resolution reanalysis with more reliable quality called ERA5 from the European Centre for Medium-Range Weather Forecasts is now available for use. ERA5 can provide global TPW data at a high temporal resolution of 1 hr and a horizontal spatial resolution of 30 km (0.25° × 0.25° in grid). ERA5 is superior compared to widely used ERA-Interim due to more data sources and new technology in data assimilation system, especially with its higher spatial and temporal resolution (Zhang et al., 2018). Since it is gap-free across the whole globe, ERA5 can be adequately collocated to different satellite sampling patterns in space and time to get the satellite-sampled data sets to construct the sampling errors in satellite data.

The ERA5 data were first collocated with COSMIC, SSMIS, and HIRS in time and space. The closest ERA5 data were collected within half an hour of the satellite observations to construct the satellite-sampled ERA5 data sets. Since the ERA5 can provide TPW with a high resolution, errors introduced from data collocation are very small (~0.01 mm). Then to quantify the sampling error in TPW from these three different satellite observations, each satellite-sampled ERA5 TPW time series was compared with the original reference TPW time series calculated from all ERA5 data. The difference between satellite-sampled TPW and reference data is defined as the sampling error. Selection of the satellites, their orbital configuration, and their scanning pattern all contribute to satellite sampling errors for climate studies (Kirk-Davidoff et al., 2005). Therefore, with this definition, satellite swath gaps, observation time differences, and missing data due to some meteorological conditions (like heavy rain, full clouds, etc.) together with the factors mentioned above will be entangled in sampling errors and automatically taken into account.

2.2. Satellite Data Preparation for Sampling Definition

2.2.1. SSMIS Data

SSMIS are satellite passive microwave radiometers carried onboard Defense Meteorological Satellite Program satellites. Microwave imagers are able to provide long-term all-sky time series of water vapor measurements (e.g., Wentz, 2015), but only over ocean owing to the complicated land surface emissivity. In addition, microwave radiation is significantly affected by heavy rain so the TPW is only retrieved under conditions of no or light to moderate rain (Elsaesser & Kummerow, 2008; Schluessel & Emery, 1990; Wentz & Spencer, 1998). In this study, the SSMIS TPW are obtained from the Remote Sensing System version 7.0 available at www.remss.com/missions/ssmi, with a resolution of 0.25° × 0.25° grid for daytime and nighttime (i.e., 1,440 × 720 × 2 per day).

2.2.2. HIRS Data

This study uses the HIRS Moisture Data Record Version 2.5 Release 2 (Borbas et al., 2005; Seemann et al., 2003, 2008), developed by Space Science and Engineering Center (SSEC) at the University of Wisconsin-Madison (UW-Madison). The data are available at SSEC ftp site (ftp://ftp.ssec.wisc.edu/pub/ICI/HIRS_TPW_GVAP_delivery_v2.5R2). TPW are determined for clear-sky radiances measured by HIRS (at 20 km for HIRS/3 and HIRS/2 and 10 km for HIRS/4 resolution) over both land and ocean for day and night. The presence of clouds in each HIRS instantaneous field of view (IFOV) is determined by collocated Advanced Very High Resolution Radiometer cloud mask, and the moisture products are only calculated when the HIRS IFOV is more than 85% clear. This process will lead to a lot of missing data in cloudy area (Udelhofen & Hartmann, 1995; van de Berg et al., 1991; Wylie et al., 2005), which will contribute to the sampling error. The long-term consistent HIRS TPW products are binned into a global map of 0.5° × 0.5° for 4 time periods daily. The HIRS data on board NOAA-15 (HIRS/3, 2007–2010), NOAA-17 (HIRS/3, 2007–2008), Metop-A (HIRS/4, 2007–2013), and Metop-B (HIRS/4, 2012–2013) are chosen in this study according to the data availability.

Table 1
Main Data Used in This Study

Data Source	Date	Coverage
ERA5	January 2007 to December 2013 from ECMWF	All-sky, global coverage; hourly data with the grid resolution of 0.25° × 0.25°; observations from various sources were assimilated
COSMIC	January 2007 to December 2013 original water vapor profiles are from CDAAC	All-sky conditions; both over land and ocean; about 200 km in horizontal resolution
SSMIS	January 2007 to December 2009 on board DMSP F16 January 2007 to December 2013 on board DMSP F17	All-sky conditions except very heavy rain; ocean only; two observations in one day for each satellite with the grid resolution of 0.25° × 0.25°
HIRS_UWisconsin	January 2007 to December 2010 on board NOAA-15 January 2007 to December 2008 on board NOAA-17 January 2007 to December 2013 on board Metop-A January 2012 to December 2013 on board Metop-B	Clear-sky only; both over land and ocean; two observations in one day for each satellite; the grid resolution is 0.5° × 0.5°;

Note. ECMWF = European Centre for Medium Range Weather Forecasts; CDAAC = Constellation Observing System for Meteorology, Ionosphere, and Climate Data Analysis and Archive Center; DMSP = Defense Meteorological Satellite Program.

2.2.3. COSMIC Data

Unlike passive microwave radiometers and infrared (IR) sensors, GPS RO is capable of using active signals to derive all-weather, high-vertical-resolution refractivity, temperature, and water vapor profiles in the neutral atmosphere (Anthes, 2011; Anthes et al., 2008). Based on this principle, satellite-based COSMIC have been launched and been in operation since June 2006. Presently, COSMIC provides about 1,800 profiles per day, with up to 90% of the total of COSMIC RO profiles reaching the lowest 2 km of the troposphere and 73% reaching the lowest 1 km (Sokolovskiy et al., 2006; Teng et al., 2013). The horizontal resolution of a COSMIC observation is about 200 km in the lower troposphere. In this study, the COSMIC reprocessed water vapor profiles are collected from COSMIC Data Analysis and Archive Center (https://cdaac-www.cosmic.ucar.edu/cdaac/products.html). To calculate COSMIC TPW, the specific humidity upward from the lowest penetration height is integrated and the water vapor amount below the lowest penetration height is compensated by using a least squares fit (Teng et al., 2013). It is shown that the calculation of TPW will become more problematic as the lowest penetration height becomes higher. Therefore, to get more available RO samples under the precondition that the RO profiles can give reasonable TPW, water vapor profiles with the lowest penetrating height of 1 km are collected to compute TPW (Teng et al., 2013). So available TPW samples are fewer than that of available water vapor profiles found in COSMIC.

The main data sets that we use to analyze the characteristics of sampling errors in this study are listed in Table 1. Note that the overlapping time period of the three satellite measurements is chosen, which is from the year of 2007 to 2013. Since the monthly mean TPW is used to determine the characteristics of sampling errors, enough samples are still obtained in 7 years.

2.3. Validation of TPW From Satellites and ERA5 Data Using Ground Based Observations

Before using the satellite data and ERA5 reanalysis to construct the global TPW time series, it is important to verify the accuracy of these TPW records. TPW data used in this study are compared with ground-based microwave radiometer (MWR) measurements from the Department of Energy Atmospheric Radiation Measurement Program (DOE/ARM) sites during the study period. ARM data are available at https://www.arm.gov/data. The ARM MWR is deployed to improve the water vapor measuring and characterize capabilities of water vapor measurements. ARM focuses on obtaining continuous TPW measurements every 20 s. In this study, three ARM permanent sites are chosen: Tropical Western Pacific site (0.521°S, 166.916°E) centered at Nauru island, Southern Great Plains site (36.606°N, 97.485°W) near Lamont in Oklahoma, and North Slope of Alaska site (71.323°N, 156.609°W) near Barrow in Alaska. The three sites are distributed in different typical latitudinal zones and have been commonly used as important and stable validation sources for spaceborne TPW measurements (Albert et al., 2005; Ferraro et al., 2005; Grody et al., 2001; Miloshevich et al., 2006; Revercomb et al., 2003).

SSMIS, HIRS, and ERA5 data within 50 km and COSMIC data within 100 km (because of the coarser resolution of COSMIC data) of the ARM MWR sites are collected. ARM MWR data within 1 hr of satellite

observations and ERA5 reanalysis are averaged to reduce the impact of different spatial scales. Additionally, to avoid the contamination effect of very heavy rain, we only use those match-up data where the cloud liquid water values are less than 0.6 mm. Figure 1 shows that all satellite data are consistent with ARM measurements, and all their linear fitting correlation coefficients are greater than 0.77. The SSMIS data, with 4,448 matches in 7 years, show a mean bias of −0.18 mm with a standard deviation (STD) of 1.79 mm, whereas larger bias and STD can be found in COSMIC and HIRS data against all three ARM sites. For COSMIC, it is partly due to very limited match numbers and the coarser spatial resolution. For HIRS, errors can mainly come from calibration issues and retrieval uncertainties. The retrieval algorithm in ARM MWR is determined by linear regression over a climatological mean condition, which might cause bias for retrievals under clear sky conditions, whereas the HIRS moisture retrieval algorithm is a statistical regression (Seemann et al., 2003, 2008) developed from an atmospheric profile database (SeeBor, Borbas et al., 2005) mainly under clear sky conditions, which might also introduce a bias. In addition, errors from data collocation/matching also contribute to these differences (e.g., HIRS data within 100 km, instead of 50 km of the ARM sites, will cause a 0.41 mm dry bias in the mean bias according to our calculations). This also suggests that a reference data set with higher spatial and temporal resolution along with good data quality should be used to reduce the error from data collocation/matching in the intercomparisons and validation. The relatively higher correlation between ERA5 TPW and ARM MWR observations can be seen in all three sites, which also proves that it is a feasible way to use ERA5 as a reference data in this study, although the temporal and spatial variabilities of ERA5 still need to be validated. The comparisons with independent ARM MWR observations indicate that all three satellite data and ERA5 reanalysis are able to construct reasonable TPW monthly mean time series.

3. Results and Analysis

3.1. Impact of Sampling Errors on TPW Variation

In this section, we attempt to show that differences in TPW time series can be created simply from inherent sampling differences of different satellite remote sensing systems. Figure 2 shows the variation of global monthly mean TPW from real satellite data (Figure 2a) and from satellite-sampled ERA5 (Figure 2b) with all ERA5 data or ERA5 ocean data (for comparison with ocean only SSMIS data) as a reference. The monthly mean TPW is calculated from all available data in the given month. In Figure 2a, TPW from different satellites shows different variabilities and magnitudes. It is hard to get a consistent and reasonable estimation with these discrepancies. In Figure 2b, we extract the sampling impact by using corresponding satellite-sampled ERA5 data. The difference between the satellite-sampled ERA5 TPW and the reference TPW from all gap-free ERA5 data is the sampling error defined in section 2.1 above. As we discussed in section 2.3, in addition to sampling errors, real satellite data also have observation errors, retrieval errors, etc. However, it can be seen from Figure 2 that when constructing the long-term TPW time series, differences among different satellite measurements are mostly attributed to their inherent sampling differences. COSMIC-sampled TPW has the largest sampling error, which is about 3 mm drier in average than that from the original ERA5, followed by HIRS, which is 1.3 mm drier in average. In contrast, the sampling error in SSMIS is small (no more than 1.5 mm) in all months. Note that since the SSMIS data are only over ocean, we only use ERA5 ocean data as reference for comparison with SSMIS-sampled TPW.

3.2. Distribution of Sampling and Sampling Errors

To find out the causes of these sampling errors in TPW time series, the distributions of sampling and sampling errors in each satellite data set are investigated. Since seasonal changes are not shown in COSMIC and SSMIS but in HIRS, only 1 month (July 2008) is shown here for COSMIC and SSMIS, but both the months of July and January are shown for HIRS. The left panel of Figure 3 shows the available sampling numbers at each grid, and right panel of Figure 3 shows the sampling errors calculated by deducting the satellite-sampled ERA5 TPW from the original ERA5 data in the same month.

Figure 3 shows that the COSMIC TPW data used in this study are mainly accumulated to middle to high latitudes (30–60°S/N), and the maximum number of observations in one grid for 1 month is about 25 (Figure 3a). Note that the grid resolution for calculating COSMIC sampling numbers is 2.5° × 2.5°, whereas that for SSMIS and HIRS is 0.5° × 0.5°. This is due to the coarser horizontal resolution of COSMIC observations. Actually, COSMIC can provide 1,800 water vapor profiles per day globally. However, when TPW is

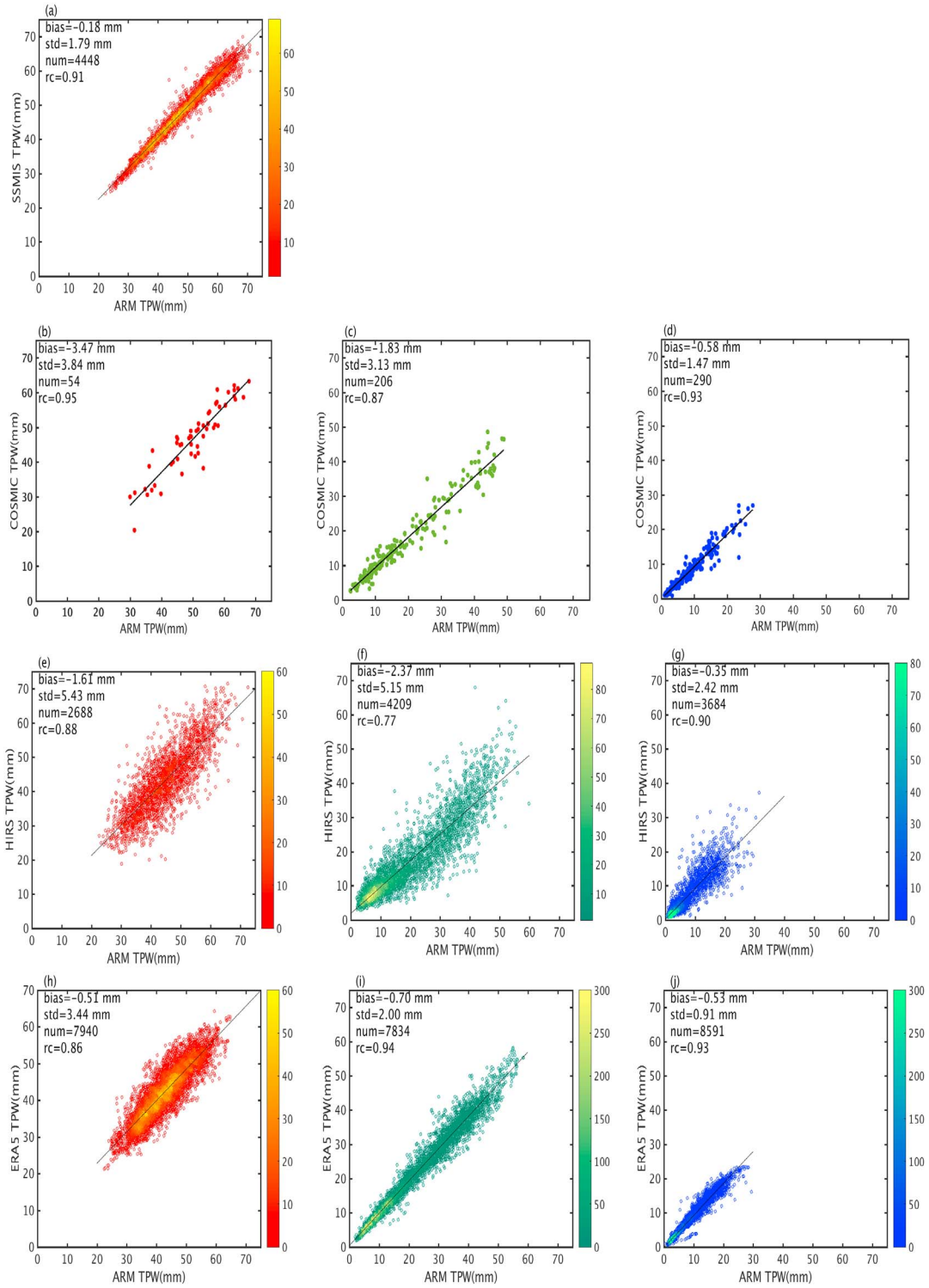

Figure 1. Scatterplots and scatter density plots for total precipitable water (TPW; mm) from real satellite data/ERA5 reanalysis data versus TPW from three Atmospheric Radiation Measurement (ARM) microwave radiometer sites. Results in Tropical Western Pacific, Southern Great Plains and North Slope of Alaska site are shown in (a), (b), (e), and (h) (red), (c), (f), and (i) (green), and (d), (g), and (j) (blue) panels, respectively. (a) TPW from Special Sensor Microwave Imager Sounder (SSMIS) data versus TWP site (ocean only); (b–d) TPW from Constellation Observing System for Meteorology, Ionosphere, and Climate (COSMIC) data versus three sites; (e–g) TPW from High-resolution Infrared Radiation Sounder (HIRS) data versus three sites; (h–j) TPW from ERA5 reanalysis versus three ARM sites are shown. Note that the scatter density plot is used for SSMIS, HIRS, and ERA5, whereas scatterplot is used for COSMIC due to limited number of matches. Satellite data compared here are from January 2007 to December 2013. ERA5 data are only from the year of 2008 due to large number of matches. In addition, the ranges of color bars are different.

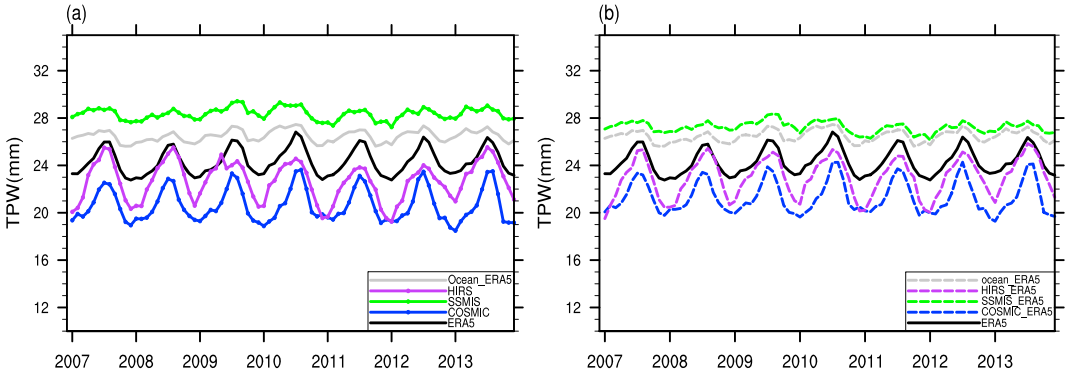

Figure 2. Time series of global monthly mean total precipitable water (TPW; mm) derived from (a) real satellite observations and (b) satellite-sampled ERA5 reanalysis, together with the original ERA5 data. The black/grey solid lines are the TPW from all ERA5/ERA5 ocean data; the variabilities of TPW from Constellation Observing System for Meteorology, Ionosphere, and Climate (COSMIC), Special Sensor Microwave Imager Sounder (SSMIS), and High-resolution Infrared Radiation Sounder (HIRS) are shown by the solid lines for real satellite data and the dashed lines for satellite-sampled ERA5 data with colors of blue, green, and purple, respectively. Note that because SSMIS TPW observations are only over the ocean, the ERA5 ocean data are used as a reference for comparisons with SSMIS.

calculated, only those water vapor profiles penetrating below 1 km are interpolated to ensure the accuracy of TPW. The interpolated TPW will become problematic when the lowest penetrating height is high since the water vapor is more concentrated in the lower troposphere. However, in tropical area, the superrefraction in boundary layer will cause many profiles to fail to reach this low level. Therefore, there will be a lack of data in tropical regions in COSMIC sampling patterns. Teng et al. (2013) also found that more than 70% of COSMIC water vapor profiles are below 1 km in middle to high latitudes and only about 10% in the tropical regions. This limited amount of available data in each grid together with the coarser horizontal resolution in COSMIC leads to a disordered and discrete distribution of sampling errors in COSMIC data, as shown in Figure 3b.

The sampling of SSMIS data is shown in Figure 3c. It is nearly uniform over global ocean area, with a range of 280–460 observations in one 0.5° × 0.5° grid. The small sampling between 30°S and 30°N is clearly shown in Figure 3c, but the number of observations (larger than 280) in these areas is still enough to sufficiently represent the monthly mean TPW. Therefore, the sampling errors of SSMIS in Figure 3d are very small, even in the area where small samples exist. These small samples are due to orbital gaps and very heavy rain in some tropical areas. By contrast, the sampling patterns and errors for HIRS are quite different. The IR sampling is not homogeneous both over land and ocean. There are more samples in subsidence areas of the Hadley/Walker circulations around subtropics and less data in Monsoon regions and the Inter Tropical Convergence Zone (ITCZ) in summer. Some persistent convective areas like some areas near the Bay of Bengal and south west of Peru even have no data for a whole month. Moreover, seasonal migration of sampling and sampling errors in HIRS is also seen due to the movement of the ITCZ. Actually, the IR sampling is good only in the dry descending areas where the cloud influence is small. Because HIRS can only provide the TPW data under clear sky conditions, the drier biases are widely spread and are larger in regions where convections are active and frequent (Figures 3f and 3h).

3.3. Statistical Characteristics of Sampling Errors

From Figure 3, it can be seen that the sampling distribution of satellite has a latitudinal dependence. Therefore, to further quantify the characteristics of sampling errors in different satellite measurements, the statistics of sampling errors are analyzed in different latitudinal zones. We choose three areas, which are north subtropical area (30°N to 60°N), tropical area (30°S to 30°N), and south subtropical area (60°S to 30°S), as they are the most important regions for water vapor distribution and variation. In addition, the TPW from polar latitudes are fairly small and the valid satellite samples are also fewer (shown in Figure 3, left panel). Both bias and root-mean-square (RMS) difference are considered to determine the sampling errors (Figure 4).

The left panel of Figure 4 shows the variation of TPW time series in the three different latitudinal zones, and the right panel of Figure 4 shows the corresponding statistics. The bias and RMS error between the satellite-

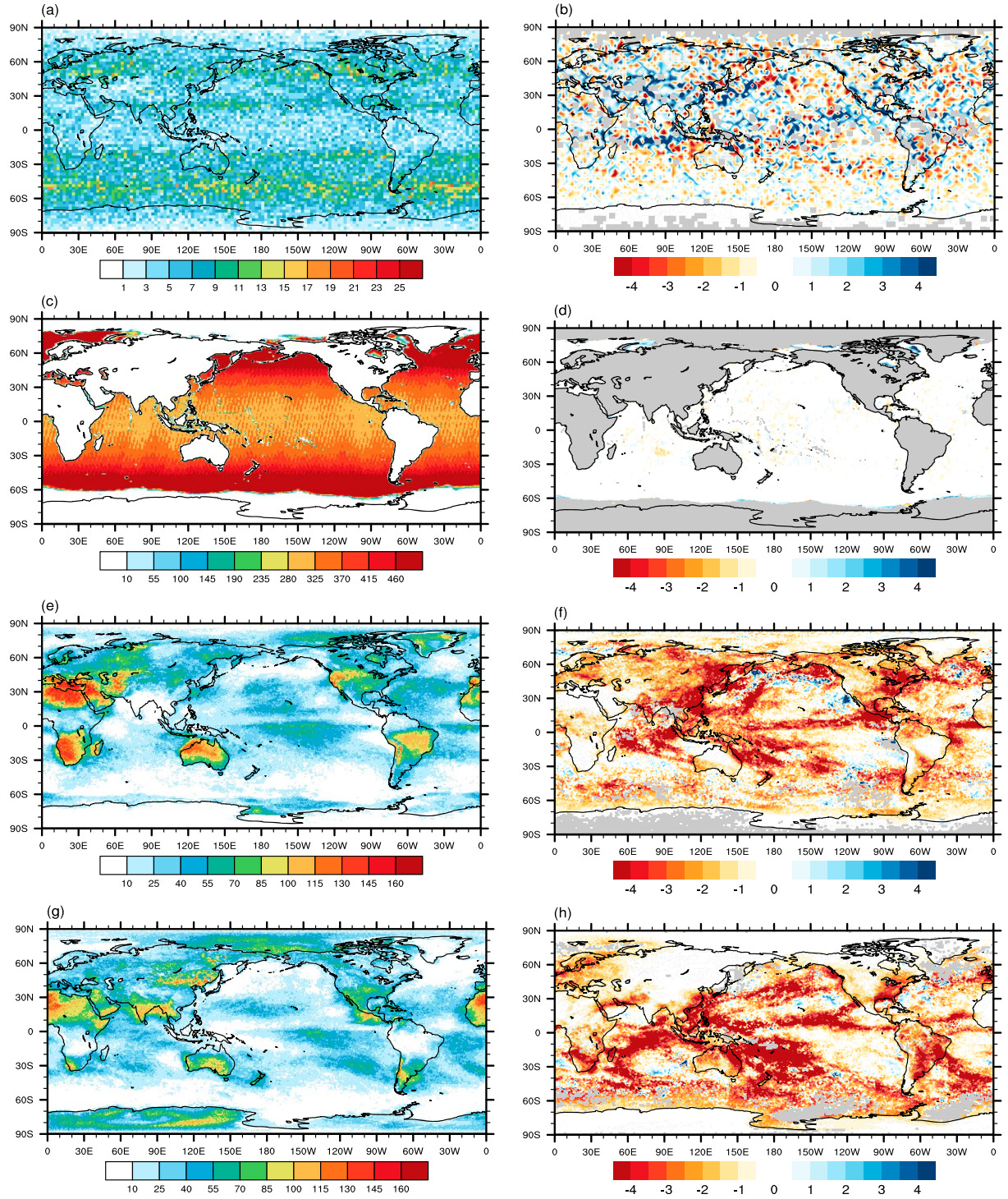

Figure 3. (a, c, e, and g) Total number of observations in each grid for a month for (a) Constellation Observing System for Meteorology, Ionosphere, and Climate (COSMIC) binned in 2.5° × 2.5° grid box in July 2008, (c) Special Sensor Microwave Imager Sounder (SSMIS) binned in 0.5° × 0.5° in July 2008, and (e and g) High-resolution Infrared Radiation Sounder (HIRS) binned in 0.5° × 0.5° in July and January 2008. Note that the ranges of the color bar are different. (b, d, f, and h) Distribution of sampling errors (mm) in the same month for (b) COSMIC, (d) SSMIS, and (f and h) HIRS at their original resolutions.

sampled ERA5 and the original ERA5 data are also provided in Table 2. For COSMIC data, the discrepancy in TPW caused by sampling errors mainly exists in tropical area where sampling numbers are small, with an averaged bias of −1.89 mm and RMS error of 1.96 mm. And TPW from COSMIC sampling has dry biases in

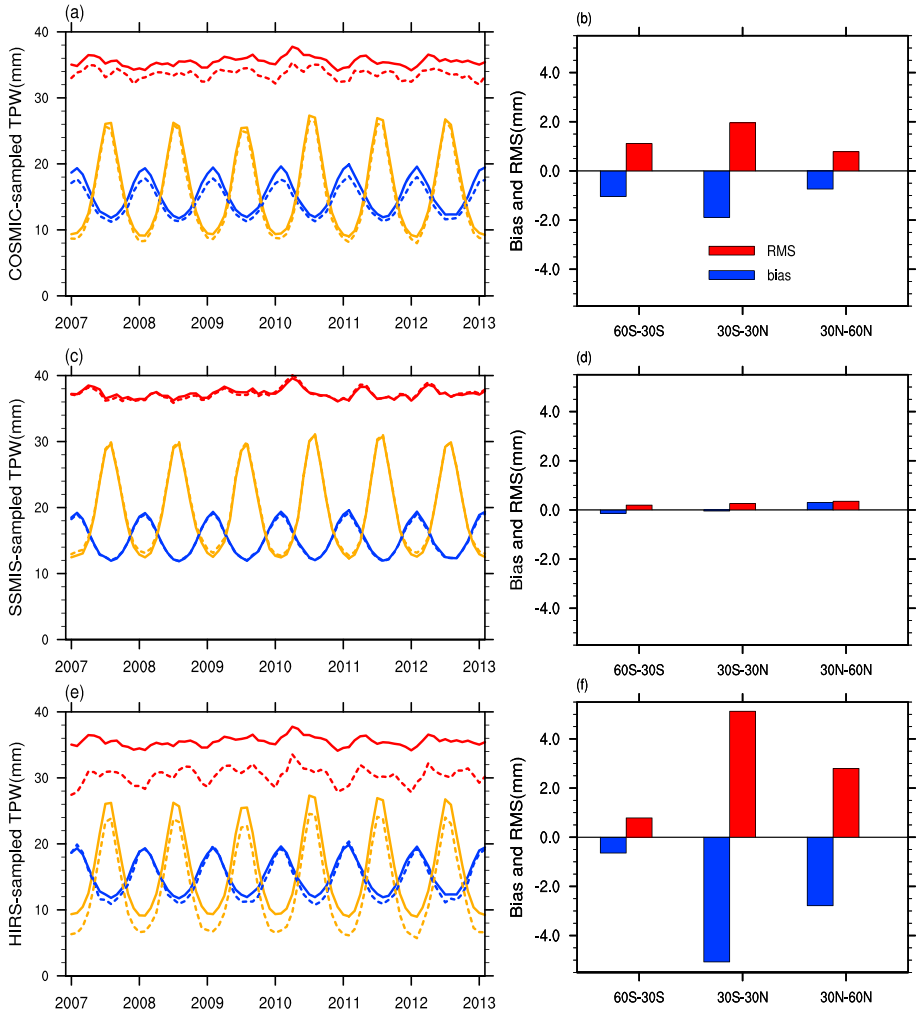

Figure 4. (a, c, and e) Total precipitable water (TPW; mm) time series in different latitudinal zones from (a) Constellation Observing System for Meteorology, Ionosphere, and Climate (COSMIC), (c) Special Sensor Microwave Imager Sounder (SSMIS), and (e) High-resolution Infrared Radiation Sounder (HIRS). Solid line is the TPW from the original ERA5 reanalysis and dashed line is the TPW from satellite-sampled ERA5 data. Latitudes from 60°S to 30°S, 30°S to 30°N, and 30°N to 60°N are indicated by colors of blue, red and yellow, respectively. (b, d, and f) Statistics (bias and root-mean-square, RMS, error) of sampling errors in corresponding regions for (b) COSMIC, (d) SSMIS, and (f) HIRS. Red char bar represents RMS error (mm) and blue char bar represents bias (mm).

all three latitudinal zones. One possible reason is that the superrefraction in the boundary layer may cause negative refractivity of RO signal, which leads to bias in retrieved humidity in the lower troposphere. Thus, the lowest penetration height in COSMIC water vapor profiles will be more often in drier regions than in

Table 2
Statistics in Different Regions From Satellite-Sampled Data

Data	COSMIC		SSMIS		HIRS	
Statistics	Bias (mm)	RMS error (mm)	Bias (mm)	RMS error (mm)	Bias (mm)	RMS error (mm)
60°S to 30°S	−1.04	1.11	−0.14	0.20	−0.64	0.79
30°S to 30°N	−1.89	1.96	−0.04	0.26	−5.07	5.12
30° to 60°N	−0.74	0.78	0.30	0.35	−2.79	2.80

Note. COSMIC = Constellation Observing System for Meteorology, Ionosphere, and Climate; SSMIS = Special Sensor Microwave Imager Sounder; HIRS = High-resolution Infrared Radiation Sounder; RMS = root-mean-square.

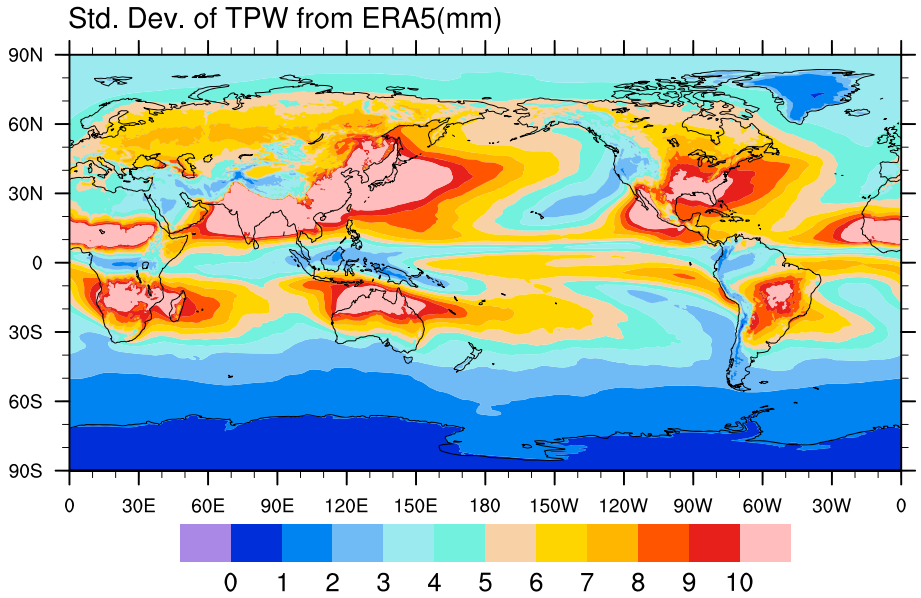

Figure 5. Standard deviation of monthly mean total precipitable water (TPW; mm) derived from ERA5 reanalysis during the study period (the year from 2007 to 2013).

wetter regions. In other words, the interpolated TPW from COSMIC will inevitably have this drier-region biased sampling. But in general, the bias and RMS error from COSMIC in different latitudinal zone are smaller than 2 mm. The sampling errors from SSMIS are very small with the largest bias value of 0.3 mm and RMS error of 0.35 mm existing in north subtropical regions where both satellite swath gaps and high TPW variability exist. Though SSMIS shows a highly stable and accurate result, it is limited to ocean and obviously fall short when it comes to global study both over land and ocean.

There are some more interesting results in HIRS sampling. As mentioned before, there are more IR samples over drier and descending areas (Figures 3e and 3g), so it is reasonable that dry biases in all three latitudinal zones are observed. However, both COSMIC and HIRS have inherent drier biased sampling globally. In particular, COSMIC has much smaller sampling numbers (~25 observations in one 2.5° × 2.5° grid) than HIRS (more than 40 observations in most 0.5° × 0.5° grids), which can be seen from Figure 3. But the bias and RMS error in COSMIC in tropical regions which is −1.89 and 1.96 mm, respectively, are both smaller than that found in HIRS, namely, −5.07 and 5.12 mm, respectively. The situation is also similar in north subtropical areas. The bias is −0.74 mm and the RMS error is 0.78 mm in COSMIC, compared with −2.79 and 2.80 mm in HIRS. In addition, there are fewer samples in HIRS in south subtropical zone, but the bias and RMS error are still smaller than those in north subtropical region where more samples exist. As mentioned before, COSMIC and HIRS both provide data over land and ocean. However, COSMIC can provide all-sky observations, whereas TPW in HIRS is highly influenced by clouds and is usually limited to clear sky only conditions. Therefore, the meteorological conditions may contribute to this issue. In tropical area, there are some convectively active regions which have more precipitation and clouds with high TPW values. Failing to detect the high TPW values in these areas creates large sampling errors in HIRS. To address the difference in subtropical regions, the TPW variability is further explored in the following section.

3.4. Dependence of Sampling Errors on TPW Variability

Figure 5 shows the distribution of the STD of monthly mean TPW from all original ERA5 data. High variabilities in TPW are found in monsoon regions and the latitudes of ITCZ tracks, whereas the small variabilities are in south subtropical regions. Since the STD is calculated from monthly mean TPW, it can reflect the seasonal changes of TPW. The monsoon area provides a typical example. In summer, the moist air from the southwest Indian Ocean and Bay of Bengal will cause torrential rainfall with cloudy-weather conditions, whereas in winter, cold and dry air from northwest Siberia and Mongolia will bring drier weather, which is usually associated with clear sky conditions. These distinct changes will cause the higher variability of

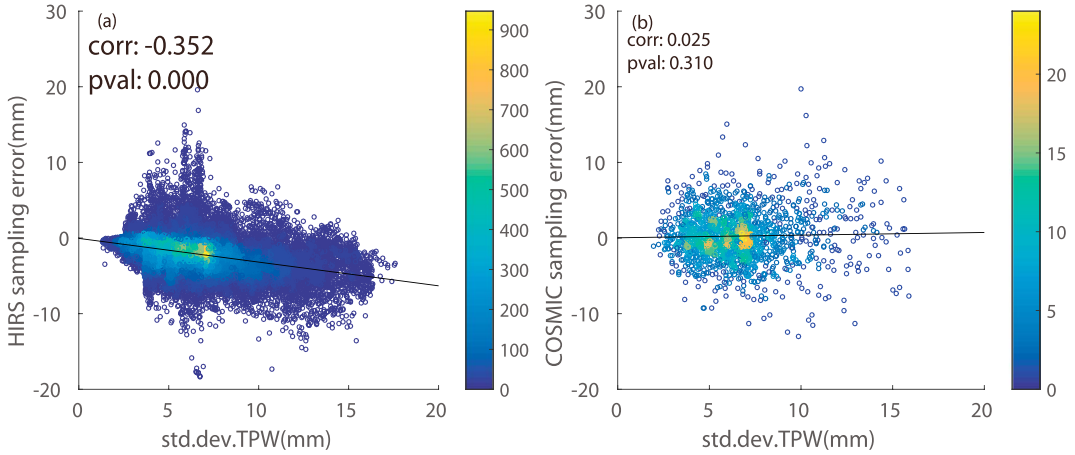

Figure 6. Scatter density plots showing the correlation between the total precipitable water (TPW; mm) variability and sampling errors (mm) from (a) High-resolution Infrared Radiation Sounder (HIRS) and (b) Constellation Observing System for Meteorology, Ionosphere, and Climate (COSMIC) in latitudes between 30°N to 60°N. The "corr" represents the correlation coefficient *R* and "pval" is the probability for significance testing.

TPW. At the same time, the clear-sky sampling in HIRS will introduce more errors by losing most of the samples with higher TPW values in cloudy skies in summer.

A correlation analysis between sampling errors and the STD of TPW is conducted for HIRS and COSMIC in all grid points in north subtropical regions. The results are in Figure 6. There is a significant correlation between sampling errors of HIRS and the standard deviation of TPW in north subtropical regions. The correlation coefficient *R* is −0.352 with a *p* value equal to 0. Whereas for COSMIC (Figure 6b), the correlation (with a *R* value of 0.025) between these two variables is not statistically significant with a *p* value of 0.310, which is larger than the 0.05 significance level. These results show that larger variability of TPW gives the potential for larger HIRS sampling errors, whereas all-sky sampling has less potential to be influenced by TPW variabilities. A similar analysis is also conducted in tropical regions (not shown here). The correlation in HIRS becomes weaker (the *R* value is −0.072) but still significant (*p* value equals to 0) compared to that from COSMIC (a *R* value of 0.032 with a *p* value of 0.063). This indicates that although we can see some seasonal changes in the distribution of HIRS sampling and sampling errors related with the movement of ITCZ (Figures 3e–3h), the dependency of sampling errors on TPW seasonal changes in tropical regions is not very clear. This result is also shown in the tropical averaged time series in Figure 4e (shown by the red lines), which is consistent with the result in John et al. (2011). In conclusion, even though HIRS data have more samples than COSMIC in tropical and north subtropical regions, they are mostly clear-sky biased thus leading to a larger deviation with reference data set ERA5. Whereas in south subtropical region, TPW have small variabilities (Figure 5), which means the TPW values in clear and cloudy skies are similar. Therefore, HIRS will have small sampling errors, which are −0.64 mm for bias and 0.79 mm for RMS error, respectively. Also, they are smaller than those sampling errors in fewer sampled COSMIC data set, which are −1.04 mm for bias and 1.11 mm for RMS error, respectively.

4. Discussions

In previous sections, the characteristics of sampling errors in COSMIC, SSMIS, and HIRS are quantified. Each of them has its strengths and limitations. It would be interesting to see if there is a method to alleviate their limitations due to inherent sampling. Tomita and Kubota (2011) assessed the efficiency of using multimicrowave sensors to reduce the sampling error caused by Sun-synchronous polar orbit satellites. They calculated the single-sampled and multisampled values of the wind speed or surface specific humidity obtained from buoy data. The multisampled values are constructed by averaging certain satellite sampled values with different combinations of microwave satellite sampling.

Based on their study, in order to further study the sampling impact on TPW analysis, the global monthly mean TPW is calculated by simply averaging multisensor sampled ERA5 data from different

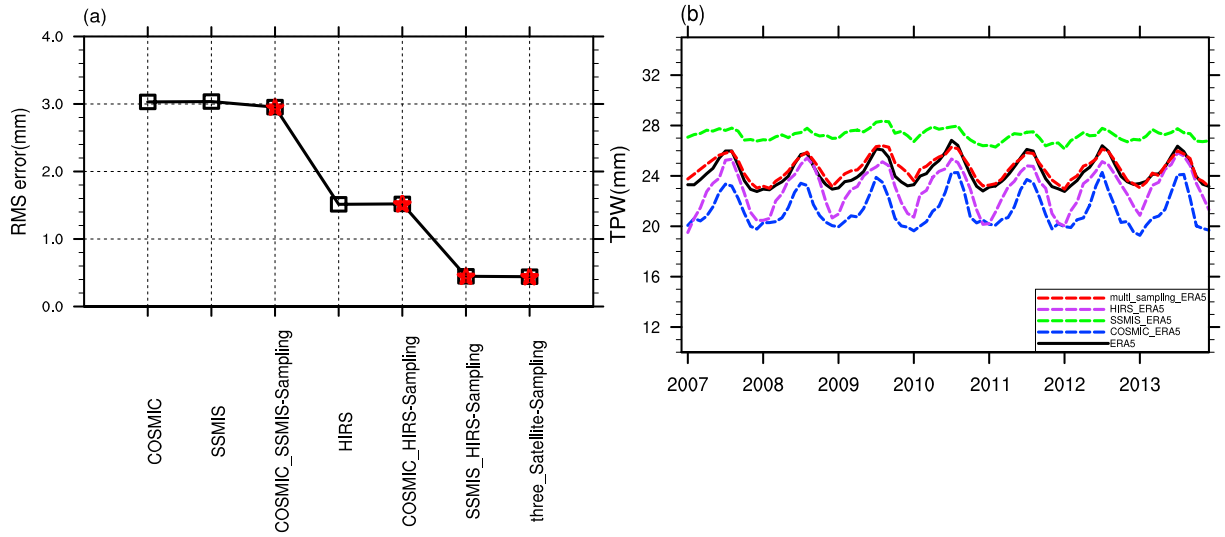

Figure 7. (a) Root-mean-square (RMS) errors (mm) of total precipitable water (TPW) monthly mean between reference values and satellite-sampled values from ERA5 in each single and multisampling pattern. Multisampling results are highlighted by red stars. (b) TPW time series similar to Figure 2b, but with one more time series indicated by red dashed line, representing the TPW values subsampled from ERA5 data with all three satellite samplings.

combinations of COSMIC, SSMIS, and HIRS sampling, after that the RMS values of all single-sampled and multisampled results are investigated to see if there is any improvement by this combination. Figure 7a shows the RMS errors, when the reference ERA5 data are compared with the subsampled ERA5 values derived from single and multisatellite samplings. Figure 7b shows the global monthly mean TPW time series similar to Figure 2b but includes one more subsampled ERA5 data sets derived from all three satellite samplings. It should be noted again that the data used here is ERA5 data with satellite samplings rather than real satellite data.

In Figure 7a, all global ERA5 data are used as the reference. The larger RMS errors are found in sparse sampled COSMIC sampling (which is 3.03 mm) and in ocean only SSMIS data (with a value of 3.04 mm), whereas the minimum RMS error (about 1.51 mm) from single sampling pattern is found in clear-sky HIRS sampling. This result seems to be contradictory to the result in sections 3.3 and 3.4 where we show that the HIRS has largest sampling errors in tropical and north subtropical areas. Actually, although COSMIC sampling is good in each latitudinal zone, the fraction of data in higher latitudes (around 60°S/N) accounts for about 70% of all available samples in COSMIC, whereas the fraction of data is 44% for tropical regions and 34% for subtropical regions in HIRS. Thus, when it comes to the calculation of global scale TPW, the higher-latitude biased sampling in COSMIC will lead to a larger RMS error compared with that from HIRS. Figure 7a also shows that RMS error will reduce if multisamplings are used compared to the corresponding single sensor sampling. When all three satellite samplings are used, the minimum RMS error of 0.44 mm will be obtained. The second least RMS error of 0.45 mm is from the combination of samplings in SSMIS and HIRS. This happened because SSMIS and HIRS have more samples globally compared with COSMIC, in particular, in tropical regions where large TPW exists. Moreover, SSMIS can provide samples over all-sky conditions, which can help to compensate the limitations of clear-sky only sampling in HIRS.

It is also shown in Figure 7b that multisensor sampled TPW time series is more consistent with the time series from reference data sets. This additional study shows that simple averaging of multisampling patterns from different satellite measurements could reduce sampling errors. However, this method cannot be used to merge real satellite data or reduce the observation errors in real satellite sensors. Because in addition to differences in sampling errors, there are also some other differences in real satellite data, like channel to channel coregistration, detector noises, time inhomogeneity caused by orbit drifting, retrieval algorithm, cloud detecting scheme, calibration, intercalibration in radiance level, and so on (Kidder & Jones, 2007; Mears et al., 2018; Schröder et al., 2016). Therefore, more sophisticated methodologies, such as the work of combining infrared and microwave measurements in Li et al. (2000), imaging and sounding (Li et al.,

2005; Li & Han, 2017), and so on, should be developed and used to fuse the multisource data for a consistent water vapor climate data record.

5. Summary and Conclusions

Satellite data are important and independent data records for global water vapor studies. Different remote sensing systems have different inherent sampling errors. In this paper, we analyzed sampling errors from three typical satellite remote sensing systems at the same time period. The three satellite observations are GPS RO data in COSMIC, microwave measurements from SSMIS and IR observations from HIRS. The ERA5 reanalysis data are used as the reference data set and are collocated with satellite observations in time and space to get the subsampled ERA5 data with the actual samplings from satellites. The difference between monthly mean TPW from satellite-sampled ERA5 reanalysis and the original ERA5 reanalysis is defined as sampling errors of satellite data. All further studies are based on this concept. The ERA5 reanalysis is chosen as the reference not because it has good performance in general but mainly because it can provide data with global coverage at high temporal and spatial resolutions. Thus, it is adequate to be subsampled by different satellite data without introducing more uncertainties from data collocation.

All TPW data used in this study are first compared with ground-based observations from ARM MWR sites. In general, satellite observations and ERA5 reanalysis data are in good agreement with the independent measurements from ARM sites, with all linear regression coefficients being more than 0.77. Nevertheless, some uncertainties remain in satellite data and reanalysis data. However, it is shown that sampling differences in COSMIC, SSMIS, and HIRS observations largely explain observed differences between associated monthly mean TPW time series.

Then the sampling patterns and sampling errors of each satellite measurements are analyzed. COSMIC samplings are biased toward middle and high latitudes (around 60°S/N). There is a lack of TPW values in tropical regions due to superrefraction in boundary layer. In general, the sparse and limited samplings in COSMIC make the distribution of sampling errors disordered. Samples in SSMIS are more uniform with small sampling errors over the ocean. There are some smaller number of samples within 30°S to 30°N due to the orbital swaths and very heavy rain. However, one obvious limitation of SSMIS sampling is that there is no information over land because microwave measurement is highly influenced by the complicated land surface emissivity. For the IR sampling in HIRS, it is more dependent on weather conditions and is good only in dry descending regions where the cloud influence is small. In general, the dry bias is spread globally.

Since the distribution of satellite samples seems to be dependent on locations, the statistical characteristics of sampling errors are further analyzed in different latitudinal zones from 60°S to 60°N. Bias and RMS error are used to determine the sampling errors in each satellite sampling. COSMIC shows drier bias in all latitudinal zones, especially in tropical regions. Because lowest penetrating height is more often in drier regions. But all bias and RMS error are smaller than 2 mm especially in higher latitudes. Sampling errors in SSMIS are smaller than 0.5 mm in all study areas with the largest one in north subtropical regions where sampling number is relatively small and high TPW variability exists. HIRS and COSMIC both have observations over land and ocean. But the IR sampling is more influenced by meteorological situations. Therefore, even though HIRS has more samplings than COSMIC, it has larger sampling errors in cloudy and rainy tropics. In addition, sampling errors in HIRS are significantly correlated with the variability of TPW, whereas all-sky sampled COSMIC results are less influenced. Higher variability of TPW can possibly cause larger sampling errors in HIRS by removing the number of samplings with high TPW values. This causes a larger discrepancy in HIRS data. But when it comes to global monthly mean TPW, because COSMIC is highly biased in higher latitudes (accounts for 70% of all available samples) where TPW is smaller than that in tropical regions, the large RMS error in COSMIC sampling will come out. Therefore, different satellite sampling has different limitations and strengths, which should be taken into account when applying the satellite data for climate studies.

In addition, an attempt is made to show the effectiveness of multisensor sampling on estimations of monthly mean TPW time series. The minimum RMS error comes from the combination of samplings from all three satellite measurements. The corresponding TPW time series also shows better agreement with that from the reference data sets. Actually, it remains a big challenge when it comes to the real satellite data merging, especially data from different sensors. This additional study shown here is not a feasible way to merge different

satellite data but just to show that sampling errors can be reduced simply by using more samplings from multisatellite measurements. In other words, if the real multisensor data can be merged adequately, combinations of their samplings will contribute to a more accurate estimation of TPW.

In conclusion, the satellite water vapor observations are typically inhomogeneous and sampling biased. Sampling differences in COSMIC, SSMIS, and HIRS observations largely explain observed differences between associated TPW time series. So it is important to take the satellite sampling into account before using satellite observations to study global TPW variation. Moreover, this preliminary work may motivate future work to reduce the sampling errors in satellite data and lead to the study on data fusion with multisatellite instruments for a more reliable and consistent water vapor climate data record.

Acknowledgments
This work is supported by research program 2018YFB0504900, NSF basic research 41775045, and China Scholarship Council (CSC; for Yunheng Xue). The ERA5 data are available at Copernicus Climate Change Service Climate Data Store (CDS); data of access are https://cds.climate.copernicus.eu/cdsapp#!/home. The COSMIC water vapor profiles are available at https://cdaac-www.cosmic.ucar.edu/cdaac/products.html. The SSMIS data are produced by Remote Sensing Systems downloaded from www.remss.com/missions/ssmi. The HIRS data are available from University of Wisconsin-Madison, Space Science and Engineering Center; the ftp site is ftp://ftp.ssec.wisc.edu/pub/ICI/HIRS_TPW_GVAP_delivery_v2.5R2. The ARM MWR data (https://www.arm.gov/data) are obtained from the Atmospheric Radiation Measurement (ARM) user facility, a U.S. Department of Energy (DOE) Office of Science User Facility managed by the Office of Biological and Environmental Research.

References

Albert, P., Bennartz, R., Preusker, R., Leinweber, R., & Fischer, J. (2005). Remote sensing of atmospheric water vapor using the Moderate Resolution Imaging Spectroradiometer. *Journal of Atmospheric and Oceanic Technology*, *22*(3), 309–314. https://doi.org/10.1175/JTECH1708.1

Allan, R. P., Ringer, M., & Slingo, A. (2003). Evaluation of moisture in the Hadley Centre climate model using simulations of HIRS water-vapour channel radiances. *Quarterly Journal of the Royal Meteorological Society: A journal of the atmospheric sciences, applied meteorology and physical oceanography*, *129*(595), 3371–3389. https://doi.org/10.1256/qj.02.217

Anthes, R. (2011). Exploring earth's atmosphere with radio occultation: Contributions to weather, climate and space weather. *Atmospheric Measurement Techniques*, *4*(6), 1077–1103. https://doi.org/10.5194/amt-4-1077-2011

Anthes, R. A., Bernhardt, P. A., Chen, Y., Cucurull, L., Dymond, K. F., Ector, D., et al. (2008). The COSMIC/FORMOSAT-3 Mission: Early results. *Bulletin of the American Meteorological Society*, *89*(3), 313–334. https://doi.org/10.1175/BAMS-89-3-313

Anthes, R. A., Rocken, C., & Kuo, Y.-H. (2000). Applications of COSMIC to meteorology and climate. *Terrestrial, Atmospheric and Oceanic Sciences*, *11*(1), 115–156. https://doi.org/10.3319/TAO.2000.11.1.115(COSMIC)

Borbas, E., Seemann, S. W., Huang, H.-L., Li, J., & Menzel, W. P. (2005). *Global profile training database for satellite regression retrievals with estimates of skin temperature and emissivity. Proc. Int. ATOVS Study Conf. XIV*, (pp. 763–770. Available online at). Beijing, China: CIMSS/University of Wisconsin—Madison. http://cimss.ssec.wisc.edu/itwg/itsc/itsc14/proceedings/2_9_Borbas.pdf

Bosilovich, M. G., Robertson, F. R., & Chen, J. (2011). Global energy and water budgets in MERRA. *Journal of Climate*, *24*(22), 5721–5739. https://doi.org/10.1175/2011JCLI4175.1

Chen, B., & Liu, Z. (2016). Global water vapor variability and trend from the latest 36 year (1979 to 2014) data of ECMWF and NCEP reanalyses, radiosonde, GPS, and microwave satellite. *Journal of Geophysical Research: Atmospheres*, *121*, 11,442–411,462. https://doi.org/10.1002/2016JD024917

Elsaesser, G. S., & Kummerow, C. D. (2008). Toward a fully parametric retrieval of the nonraining parameters over the global oceans. *Journal of Applied Meteorology and Climatology*, *47*(6), 1599–1618. https://doi.org/10.1175/2007jamc1712.1

Erlick, C., & Ramaswamy, V. (2003). Note on the definition of clear sky in calculations of shortwave cloud forcing. *Journal of Geophysical Research*, *108*(D5), 4156. https://doi.org/10.1029/2002JD002990

Ferraro, R., Weng, F., Grody, C., Zhao, N., Meng, L., Kongoli, H., et al. (2005). NOAA operational hydrological products derived from the AMSU. *IEEE Transactions on Geoscience and Remote Sensing*, *43*(5), 1036–1049. https://doi.org/10.1109/TGRS.2004.843249

Grody, N., Zhao, J., Ferraro, R., Weng, F., & Boers, R. (2001). Determination of precipitable water and cloud liquid water over oceans from the NOAA 15 advanced microwave sounding unit. *Journal of Geophysical Research*, *106*(D3), 2943–2953. https://doi.org/10.1029/2000JD900616

Ho, S., Hunt, D., Steiner, A. K., Mannucci, A. J., Kirchengast, G., Gleisner, H., et al. (2012). Reproducibility of GPS radio occultation data for climate monitoring: Profile-to-profile inter-comparison of CHAMP climate records 2002 to 2008 from six data centers. *Journal of Geophysical Research*, *117*, D18111. https://doi.org/10.1029/2012JD017665

Ho, S.-P., Kuo, Y.-H., & Sokolovskiy, S. (2007). Improvement of the temperature and moisture retrievals in the lower troposphere using AIRS and GPS radio occultation measurements. *Journal of Atmospheric and Oceanic Technology*, *24*(10), 1726–1739. https://doi.org/10.1175/JTECH2071.1

Ho, S.-P., & Peng, L. (2018). Global water vapor estimates from measurements from active GPS RO sensors and passive infrared and microwave sounders.

Ho, S.-P., Peng, L., Mears, C., & Anthes, R. A. (2017). Comparison of global observations and trends of total precipitable water derived from microwave radiometers and COSMIC radio occultation from 2006 to 2013. *Atmospheric Chemistry and Physics Discussions*, *18*(1), 1–44. https://doi.org/10.5194/acp-2017-525

Ho, S.-P., Zhou, X., Kuo, Y.-H., Hunt, D., & Wang, J.-H. (2010). Global evaluation of radiosonde water vapor systematic biases using GPS radio occultation from COSMIC and ECMWF analysis. *Remote Sensing*, *2*(5), 1320–1330. https://doi.org/10.3390/rs2051320

Huang, C. Y., Teng, W. H., Ho, S. P., & Kuo, Y. H. (2013). Global variation of COSMIC precipitable water over land: Comparisons with ground-based GPS measurements and NCEP reanalyses. *Geophysical Research Letters*, *40*, 5327–5331. https://doi.org/10.1002/grl.50885

Iacono, M. J., Delamere, J. S., Mlawer, E. J., & Clough, S. A. (2003). Evaluation of upper tropospheric water vapor in the NCAR Community Climate Model (CCM3) using modeled and observed HIRS radiances. *Journal of Geophysical Research*, *108*(D2), 4037. https://doi.org/10.1029/2002JD002539

John, V., & Soden, B. J. (2007). Temperature and humidity biases in global climate models and their impact on climate feedbacks. *Geophysical Research Letters*, *34*, L18704. https://doi.org/10.1029/2007GL030429

John, V. O., Holl, G., Allan, R. P., Buehler, S. A., Parker, D. E., & Soden, B. J. (2011). Clear-sky biases in satellite infrared estimates of upper tropospheric humidity and its trends. *Journal of Geophysical Research*, *116*, D14108. https://doi.org/10.1029/2010JD015355

Kawanishi, T., Sezai, T., Ito, Y., Imaoka, K., Takeshima, T., Ishido, Y., et al. (2003). The Advanced Microwave Scanning Radiometer for the Earth Observing System (AMSR-E), NASDA's contribution to the EOS for global energy and water cycle studies. *IEEE Transactions on Geoscience and Remote Sensing*, *41*(2), 184–194. https://doi.org/10.1109/TGRS.2002.808331

Kelly, G. (1997). Influence of observations on the operational ECMWF system. *Bulletin of the World Meteorological Organization*, *46*(4), 336–341.

Kidder, S. Q., & Jones, A. S. (2007). A blended satellite total precipitable water product for operational forecasting. *Journal of Atmospheric and Oceanic Technology*, *24*(1), 74–81. https://doi.org/10.1175/JTECH1960.1

Kirk-Davidoff, D. B., Goody, R. M., & Anderson, J. G. (2005). Analysis of sampling errors for climate monitoring satellites. *Journal of Climate*, *18*(6), 810–822. https://doi.org/10.1175/JCLI-3301.1

Kursinski, E., & Hajj, G. (2001). A comparison of water vapor derived from GPS occultations and global weather analyses. *Journal of Geophysical Research*, *106*(D1), 1113–1138. https://doi.org/10.1029/2000JD900421

Li, J., & Han, W. (2017). A step forward toward effectively using hyperspectral IR sounding information in NWP. *Advances in Atmospheric Sciences*, *34*(11), 1263–1264. https://doi.org/10.1007/s00376-017-7167-2

Li, J., Liu, C.-Y., Huang, H.-L., Schmit, J., Wu, T., Paul, X., et al. (2005). Optimal cloud-clearing for AIRS radiances using MODIS. *IEEE Transactions on Geoscience and Remote Sensing*, *43*(6), 1266–1278.

Li, J., Wang, P., Han, H., Li, J., & Zheng, J. (2016). On the assimilation of satellite sounder data in cloudy skies in numerical weather prediction models. *Journal of Meteorological Research*, *30*(2), 169–182. https://doi.org/10.1007/s13351-016-5114-2

Li, J., Wolf, W. W., Menzel, W. P., Zhang, W., Huang, H.-L., & Achtor, T. H. (2000). Global soundings of the atmosphere from ATOVS measurements: The algorithm and validation. *Journal of Applied Meteorology*, *39*(8), 1248–1268. https://doi.org/10.1175/1520-0450(2000)039<1248:GSOTAF>2.0.CO;2

Marks, D., Winstral, A., Flerchinger, G., Reba, M., Pomeroy, J., Link, T., & Elder, K. (2008). Comparing simulated and measured sensible and latent heat fluxes over snow under a pine canopy to improve an energy balance snowmelt model. *Journal of Hydrometeorology*, *9*(6), 1506–1522. https://doi.org/10.1175/2008JHM874.1

Mears, C. A., Smith, D. K., Ricciardulli, L., Wang, J., Huelsing, H., & Wentz, F. J. (2018). Construction and uncertainty estimation of a satellite-derived total precipitable water data record over the world's oceans. *Earth and Space Science*, *5*(5), 197–210. https://doi.org/10.1002/2018EA000363

Mears, C. A., Smith, D. K., & Wentz, F. J. (2015). Estimated errors in retrievals of ocean parameters from SSMIS. *Journal of Geophysical Research: Atmospheres*, *120*, 5816–5830. https://doi.org/10.1002/2014JD023049

Mears, C. A., Wang, J., Smith, D., & Wentz, F. J. (2015). Intercomparison of total precipitable water measurements made by satellite-borne microwave radiometers and ground-based GPS instruments. *Journal of Geophysical Research: Atmospheres*, *120*, 2492–2504. https://doi.org/10.1002/2014JD022694

Mears, C. A., Wentz, F. J., Thorne, P., & Bernie, D. (2011). Assessing uncertainty in estimates of atmospheric temperature changes from MSU and AMSU using a Monte-Carlo estimation technique. *Journal of Geophysical Research*, *116*, D08112. https://doi.org/10.1029/2010JD014954

Menzel, W. P., Holt, F. C., Schmit, T. J., Aune, R. M., Schreiner, A. J., Wade, G. S., & Gray, D. G. (1998). Application of GOES-8/9 soundings to weather forecasting and nowcasting. *Bulletin of the American Meteorological Society*, *79*(10), 2059–2077. https://doi.org/10.1175/1520-0477(1998)079<2059:AOGSTW>2.0.CO;2

Menzel, W. P., Schmit, T. J., Zhang, P., & Li, J. (2018). Satellite-based atmospheric infrared sounder development and applications. *Bulletin of the American Meteorological Society*, *99*(3), 583–603. https://doi.org/10.1175/bams-d-16-0293.1

Miloshevich, L. M., Vömel, H., Whiteman, D. N., Lesht, B. M., Schmidlin, F. J., & Russo, F. (2006). Absolute accuracy of water vapor measurements from six operational radiosonde types launched during AWEX-G and implications for AIRS validation. *Journal of Geophysical Research*, *111*, D09S10. https://doi.org/10.1029/2005JD006083

Purdom, J. F., & Menzel, W. P. (1996). *Evolution of satellite observations in the United States and their use in meteorology Historical Essays on Meteorology 1919–1995*, (pp. 99–155). Boston, MA: Springer.

Revercomb, H. E., Turner, D. D., Tobin, D. C., Knuteson, R. O., Feltz, W. F., Barnard, J., et al. (2003). The arm program's water vapor intensive observation periods. *Bulletin of the American Meteorological Society*, *84*(2), 217–236. https://doi.org/10.1175/BAMS-84-2-217

Schluessel, P., & Emery, W. J. (1990). Atmospheric water vapour over oceans from SSM/I measurements. *International Journal of Remote Sensing*, *11*(5), 753–766. https://doi.org/10.1080/01431169008955055

Schröder, M., Lockhoff, M., Forsythe, J. M., Cronk, H. Q., Vonder Haar, T. H., & Bennartz, R. (2016). The GEWEX water vapor assessment: Results from intercomparison, trend, and homogeneity analysis of total column water vapor. *Journal of Applied Meteorology and Climatology*, *55*(7), 1633–1649. https://doi.org/10.1175/JAMC-D-15-0304.1

Seemann, S. W., Borbas, E. E., Knuteson, R. O., Stephenson, G. R., & Huang, H.-L. (2008). Development of a global infrared land surface emissivity database for application to clear sky sounding retrievals from multispectral satellite radiance measurements. *Journal of Applied Meteorology and Climatology*, *47*(1), 108–123. https://doi.org/10.1175/2007JAMC1590.1

Seemann, S. W., Li, J., Menzel, W. P., & Gumley, L. E. (2003). Operational retrieval of atmospheric temperature, moisture, and ozone from MODIS infrared radiances. *Journal of Applied Meteorology*, *42*(8), 1072–1091. https://doi.org/10.1175/1520-0450(2003)042<1072:OROATM>2.0.CO;2

Shi, L., & Bates, J. J. (2011). Three decades of intersatellite-calibrated High-Resolution Infrared Radiation Sounder upper tropospheric water vapor. *Journal of Geophysical Research*, *116*, D04108. https://doi.org/10.1029/2010JD014847

Soden, B. J., & Held, I. M. (2006). An assessment of climate feedbacks in coupled ocean–atmosphere models. *Journal of Climate*, *19*(14), 3354–3360. https://doi.org/10.1175/JCLI3799.1

Soden, B. J., Wetherald, R. T., Stenchikov, G. L., & Robock, A. (2002). Global cooling after the eruption of Mount Pinatubo: A test of climate feedback by water vapor. *Science*, *296*(5568), 727–730. https://doi.org/10.1126/science.296.5568.727

Sohn, B.-J., Schmetz, J., Stuhlmann, R., & Lee, J.-Y. (2006). Dry bias in satellite-derived clear-sky water vapor and its contribution to longwave cloud radiative forcing. *Journal of Climate*, *19*(21), 5570–5580. https://doi.org/10.1175/JCLI3948.1

Stephens, G. L., Randall, D. A., Wittmeyer, I. L., Dazlich, D. A., & Tjemkes, S. (1993). The Earth's radiation budget and its relation to atmospheric hydrology: 3. Comparison of observations over the oceans with a GCM. *Journal of Geophysical Research*, *98*(D3), 4931–4950. https://doi.org/10.1029/92JD02520

Sokolovskiy, S., Kuo, Y.-H., Rocken, C., Schreiner, W. S., Hunt, D., & Anthes, R. A. (2006). Monitoring the atmospheric boundary layer by GPS radio occultation signals recorded in the open-loop mode. *Geophysical Research Letters*, *33*, L12813. https://doi.org/10.1029/2006GL025955

Teng, W.-H., Huang, C.-Y., Ho, S.-P., Kuo, Y.-H., & Zhou, X.-J. (2013). Characteristics of global precipitable water in ENSO events revealed by COSMIC measurements. *Journal of Geophysical Research: Atmospheres*, *118*, 8411–8425. https://doi.org/10.1002/jgrd.50371

Tomita, H., & Kubota, M. (2011). Sampling error of daily mean surface wind speed and air specific humidity due to Sun-synchronous satellite sampling and its reduction by multi-satellite sampling. *International Journal of Remote Sensing*, *32*(12), 3389–3404. https://doi.org/10.1080/01431161003749428

Trenberth, K. E., Fasullo, J., & Smith, L. (2005). Trends and variability in column-integrated atmospheric water vapor. *Climate Dynamics*, *24*(7-8), 741–758. https://doi.org/10.1007/s00382-005-0017-4

Udelhofen, P. M., & Hartmann, D. L. (1995). Influence of tropical cloud systems on the relative humidity in the upper troposphere. *Journal of Geophysical Research*, *100*(D4), 7423–7440. https://doi.org/10.1029/94JD02826

van de Berg, L., Pyomjamsri, A., & Schmetz, J. (1991). Monthly mean upper tropospheric humidities in cloud-free areas from Meteosat observations. *International Journal of Climatology*, *11*(8), 819–826. https://doi.org/10.1002/joc.3370110802

Wagner, T., Beirle, S., Grzegorski, M., & Platt, U. (2006). Global trends (1996–2003) of total column precipitable water observed by Global Ozone Monitoring Experiment (GOME) on ERS-2 and their relation to near-surface temperature. *Journal of Geophysical Research*, *111*, D12102. https://doi.org/10.1029/2005JD006523

Wentz, F. J. (1997). A well-calibrated ocean algorithm for special sensor microwave/imager. *Journal of Geophysical Research*, *102*(C4), 8703–8718. https://doi.org/10.1029/96JC01751

Wentz, F. J. (2015). A 17-yr climate record of environmental parameters derived from the Tropical Rainfall Measuring Mission (TRMM) Microwave Imager. *Journal of Climate*, *28*(17), 6882–6902. https://doi.org/10.1175/JCLI-D-15-0155.1

Wentz, F. J., & Spencer, R. W. (1998). SSM/I rain retrievals within a unified all-weather ocean algorithm. *Journal of the Atmospheric Sciences*, *55*(9), 1613–1627. https://doi.org/10.1175/1520-0469(1998)055<1613:SIRRWA>2.0.CO;2

Wylie, D., Jackson, D. L., Menzel, W. P., & Bates, J. J. (2005). Trends in global cloud cover in two decades of HIRS observations. *Journal of Climate*, *18*(15), 3021–3031. https://doi.org/10.1175/JCLI3461.1

Zhang, Q., Ye, J., Zhang, S., & Han, F. (2018). Precipitable water vapor retrieval and analysis by multiple data sources: Ground-based GNSS, radio occultation, radiosonde, microwave satellite, and NWP reanalysis data. *Journal of Sensors*, *2018*, 1–13. https://doi.org/10.1155/2018/3428303